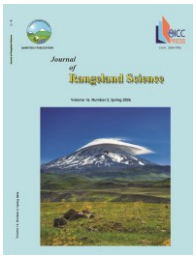

J. Rangeland Sci., 2026; 16(2): 123-136

Journal of Rangeland Science (JRS)

https://doi.org/10.57647/JRS.2026.1602.12

Research Article

A Training Sample Migration Method for Classification of Vegetation Cover Using LSTM Model and Remote Sensing Data (Case Study: Ravansar County, Kermanshah Province, Iran)

Moslem Hadidi, Alireza Shakiba*, Ali Akbar Matkan

Remote Sensing & GIS Research Center, Faculty of Earth Sciences, Shahid Beheshti University, Tehran, Iran

***Corresponding author:** a-shakiba@sbu.ac.ir

Article History:

Received:
06 August 2024

Revised:
01 January 2025

Accepted:
17 February 2025

Published in Issue:
30 June 2026

Abstract

Improving the quality of land-use change classification, with an emphasis on rangeland vegetation, by using time-series satellite imagery and migration data for training can lead to proper management of natural lands. Rangelands, as one of the most important ecosystems on Earth, play a crucial role in maintaining ecological balance and ensuring food security. Training data (reference data) are a fundamental factor in determining the quality of information generated by machine learning methods, as they serve as the basis for future decisions. Using training data migration methods helps reduce data collection costs and enables timely access to reliable training data. This study aims to improve classification quality by applying a training data transfer technique based on an artificial intelligence algorithm, Sentinel-2 satellite image time-series data, and distance-based criteria. The study area is located in Ravansar, Kermanshah province, in the west of Iran. Ravansar has various biological regions involving urban areas, agricultural farms, rangelands and geological formations. To this end, migration data samples from 2017 to 2021 were determined to promote the accuracy of vegetation cover classification using three methods include Euclidean Distance (ED), Spectral Angle Distance (SAD) and Dynamic Time Warping (DTW). This research indicated that the vegetation plant classes require more time data, while other classes need no time series. In addition, using the remote sensing data of the Sentinel-2 sensor for the migration of training samples indicated the efficiency of the proposed methods for producing up-to-date maps without extensive land surveys. The proposed algorithm, using DTW, SAD, and ED flexible distance measures, Sentinel-2 image time series data, and providing optimal thresholds for different feature spaces, achieved an accuracy of up to 76%. This capability, the ability to extract useful information from multi-temporal data of the Sentinel-2 sensor without the need to use the entire time interval, is an important advantage. This method provides valuable insights into changes and dynamics of plant cover, as well as the identification and classification of vegetation, which are essential for the optimal management of natural resources and food security. The final map, incorporating plant cover and other land-use classes, serves as a practical tool for monitoring annual vegetation changes and assessing ecological shifts, thereby supporting policymakers and researchers in strategic planning and management.

Keywords: Classification, Training data migration, Distance criterion, Deep learning, Climate changes, Remote sensing

Cite this article: Hadidi, M., Shakiba, A. & Matkan, A.A., (2026). *Journal of Rangeland Science* , A Training Sample Migration Method for Classification of Vegetation Cover Using LSTM Model and Remote Sensing Data (Case Study: Ravansar County, Kermanshah Province, Iran)*, 16(2),* 123-136. https://doi.org/10.57647/jrs.2026.1602.12

1. Introduction

Natural resources cover almost one-third of the earth's surface and exist in all the continents except Antarctica (Reynolds et al., 2009; White, 2000). Rangelands directly ensure the food security and help the livelihood of almost one billion people all over the world (FAO, 2010). The most important services of rangelands are to absorb Carbon, create biodiversity, purify water, and control soil erosion (Gibon, 2005; White, 2000). Since the Rangelands cover a wide area around the world, they absorb almost 50% more carbon than the forests (Conant, 2010). Severe weather conditions, especially droughts, can damage the range quality and reduce the range productivity (Reichstein et al., 2007). Moreover, they are regarded as valuable for numerous bird and insect species (Hilpold et al., 2018; Lengyel et al., 2016). The necessity to monitor the environment is undeniable due to the continuous decline in biodiversity, water shortage, and land degradation caused by human activities and climate change. Land degradation and biodiversity loss in dry and semi-dry areas like Iran are considerably important (Reinermann et al., 2020).

Remote sensing science extracts valuable information without making physical contact with the object. This trend includes the data acquisition by the sensors and magnetic reflection storage from the Earth's surface. The sensors are often installed on the satellite, and aerial platforms, as well as drones (Delince et al., 2017). Nowadays, different methods are developed to describe the Earth's surface features with respect to unprecedented progress in information technology and monitoring capabilities. The information achieved by remote sensing data to be used in a variety of fields such as environmental monitoring, urban planning, agriculture, forestry, water resources management, and meteorology. Therefore, understanding the various concepts in the desired field and infrastructure limitations is important for the correct use (Rußwurm & Körner, 2020).

Over the past decade, remote sensing data have been used to map the plant covers with really high spatial resolution (Guo et al., 2017). Lots of studies have shown that plant classes like forests, shrubs, and Rangelands may be extracted using multispectral images with high precision (Rapinel et al., 2018). However, plant classes often involve plenty of plant species distributed on the basis of such environmental variables as soil moisture and weather conditions (Mariotto et al., 2013). Consequently, classic mapping of plant species types cannot be used to monitor the natural ecosystems and environment because many plant areas have been merged (Rapinel et al., 2018). Using the machine learning approaches along with remote sensing data can be a suitable solution to monitor and manage the environmental resources in one region.

In machine learning techniques, training data are the fundamental element in determining the quality of the information achieved, as these data form the basis for future decisions. Training data inevitably affect model precision, reliability, and predictive power, as well as the algorithm's ability to adapt to new environments. Also, uncertainty in reference samples and a small number of samples are considered as the main error sources in the monitored algorithms (Ghorbanian et al., 2021). On the other hand, periodic and regular collection of reference samples requires lots of time and costs, which does not seem operational.

Training samples represent the true land-cover classes on the Earth's surface. When significant changes do not occur in spectral, spatial, and structural features, these samples remain applicable over time. This assumption forms the basis of many change-detection methods. In such methods, data from specific time periods are often compared at the pixel level, and changed areas are identified based on predefined thresholds. This approach can be used to migrate training samples from a source time to a target time. Thus, if training samples remain unchanged during the period of interest, they can be used as reliable ground-truth data. Using the approaches of training data migration contributes to decreasing the data collection costs and having timely access to reliable training data at the appropriate time (Fekri et al., 2021).

Considering the novelty of the training data migration discussion, few studies have been conducted in this regard and in the following, the relevant studies are addressed:

Ghorbanian et al. (2020) in a study provided the map of land use in 13 general classes such as water, clay soil, salty soil and forest using the cloud computing system of Google Earth Engine (GEE). The used data included the optical multispectral images with the Sentinel-2 10 m spatial resolution limit and SAR data of the Sentinel-2 sensor. Applying the random forest algorithm, a total precision of 91.35% has been achieved

In another study done by Zhang et al. (2023) in Hailon, China, the Sentinel-2 time series and data of reference samples during 2017, 2018 and 2020 were used to provide a land use map with the classes of rice, corn and soybean in the target year (2020). According to five spectral indices involving GCVI, MNDWI, LSWI, NDVI and NDRI, and DTW, the similarities between two time series data with different lengths were measured. Results indicated that the distance criterion had a high capability in time adjustment of input vectors and the achieved map by the random forest had a total accuracy of 95% based on the transferred data Fekri et al. (2021) presented

10.57647/jrs.2026.1602.12

a classification method based on the existing samples in the reference year (2020) for the Shadgan wetland, Khuzestan province, Iran. Using spectral indices, Euclidean distance criteria and spectral angular ones, the available samples have been transferred to three target years (2018, 2019 & 2021) and afterwards, the land use types have been classified into 9 classes on the GEE platform using the random forest method. The suggested method in this article could achieve a total precision of 97% in the reference year and 81% in the target years.

Mao et al.(2020) developed a theme map for the Chinese wetlands by an object-based hybrid and hierarchical classification method. In the study, the mapped information of the years 2014 and 2016 was used to give the map of wetlands in 2020.

2. Materials and methods

2.1. The used data and case study

The study area is located in Ravansar, Kermanshah province, in the west of Iran. Ravansar has various biological regions involving urban areas, agricultural farms, rangelands and geological formations. The used reference data have been extracted from the research conducted by Ghorbanian et al. (2020), which was a land cover classification map with an accuracy of 91% for 2017. This map operated as a basis for the algorithm of training sample data and presented valuable insights into the distribution of plant covers in that period. The data set used for the training and analysis included nine separate classes, like urban areas, rangelands, agricultural lands, wetlands, clay, water, sand, and outcrop. These classes reflect the environmental biodiversity and land uses from the structures constructed by human beings to natural properties. Table 1 presents the ground reality data of the case study. Putting these nine classes in the algorithm of training samples migration data comprehensively involves all the land use covers in Ravansar and facilitates the exact analysis of land use changes over time. Figure 1 shows the location of the study area and the distribution of ground reality data extracted in 2017. In this article, the time series images of the Sentinel-2 sensor were used, from 2017 and 2021. In 2017, a total of 14 images were taken in this area without the presence of clouds and were selected close in time to the 2021 images.

2.2. Research Method

In this research, early classification is introduced as one of the key solutions to accelerate and improve the efficiency of the monitoring process. This method enables the classification model to recognize land-cover types and changes by observing only a portion of the time series. To achieve this goal, end-to-end deep learning algorithms are employed to transform input data of varying lengths into a fixed-length latent representation, eliminating the need for a fixed-length time series. The feature allows the model can give more accurate results using the features of time series variables while classifying and updating the maps. As well, using the recurrent (Rußwurm & Körner, 2018) and self-attention (Garnot et al., 2020) networks considerably reduced the classification error in order to create a flexible feature space.

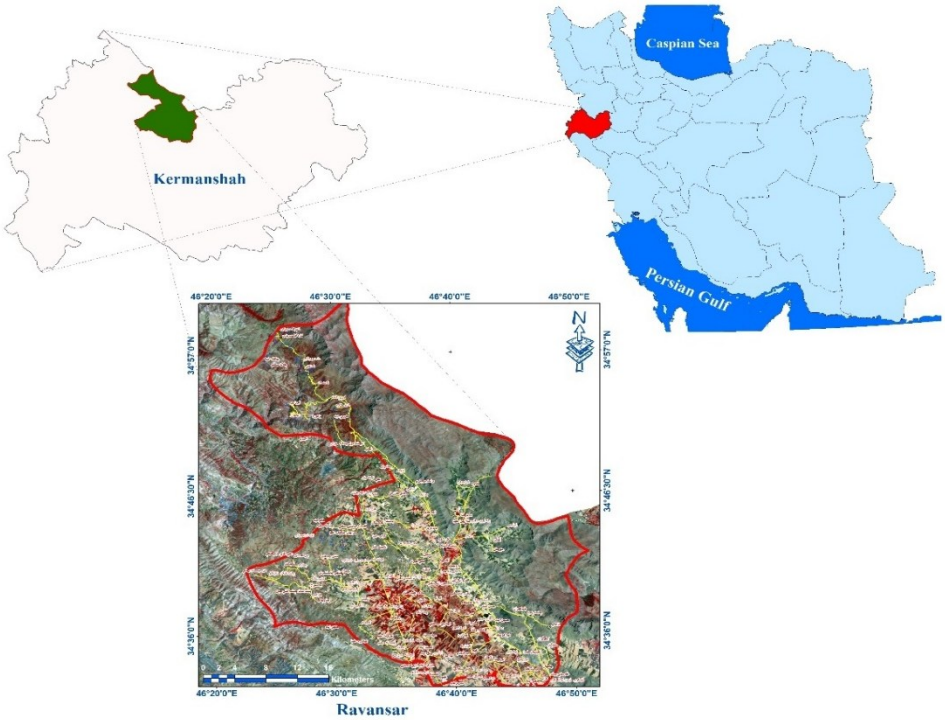

Figure 1. Map of the study area in Ravansar County, Kermanshah province, Iran, in 2017

10.57647/jrs.2026.1602.12

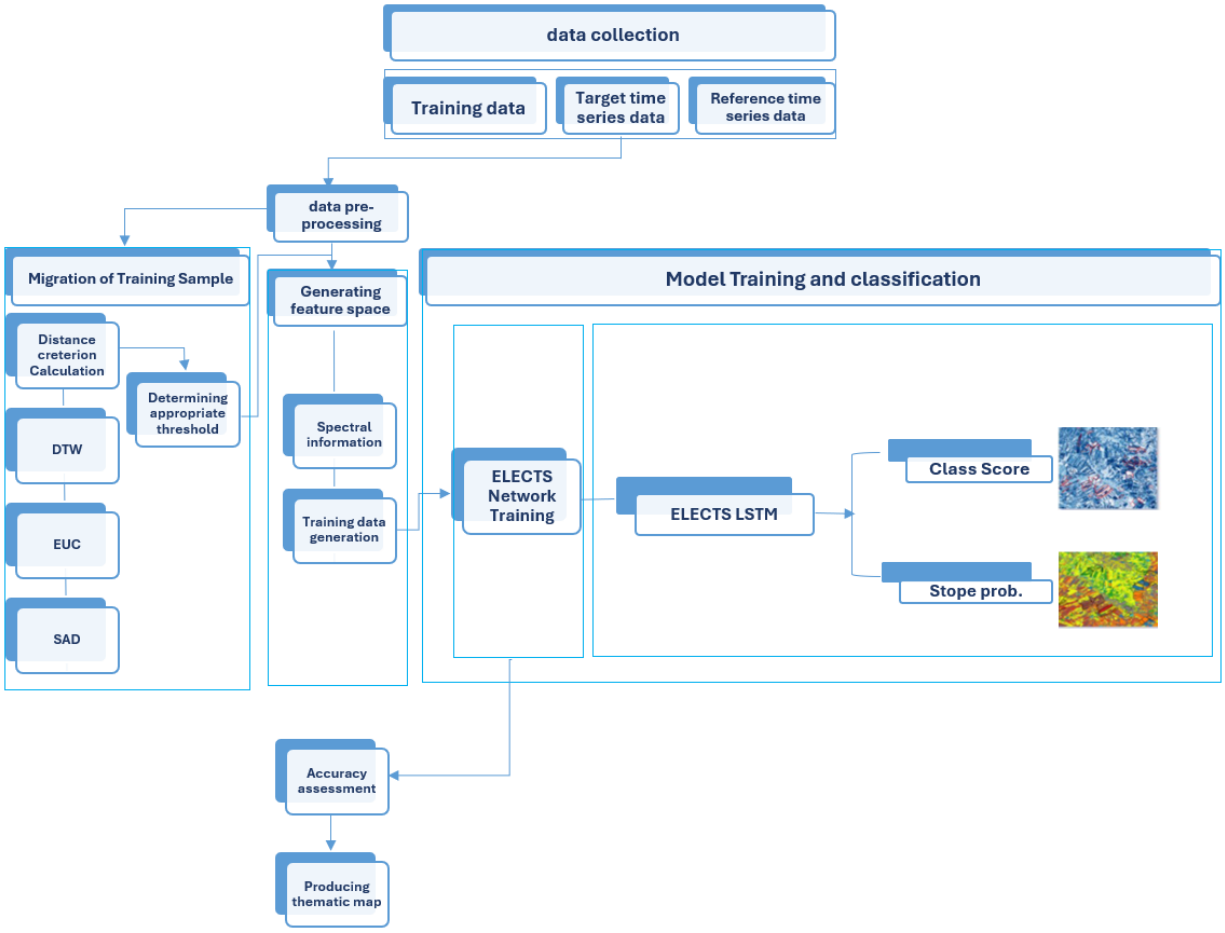

Figure 2. Flowchart of study steps

Table 1. Characteristics of land use in Ravansar in 2017

Class	Number of samples	Number of polygons
Urban	42330	1
Rangelands	80760	50
Farmland	139857	353
Wetland	6010	120
Kalut	10722	244
Clay	5125	66
Outcrop	52563	24
Sand	17166	349
Water	2406	3
Total classes	356939	1220

To enhance the accuracy and reliability of updated plant cover maps, multiple criteria were applied to compute the distance and guide the migration of training samples. These criteria include advanced metrics such as dynamic time warping and spectral angle, which were rigorously evaluated for training sample migration and feature classification. In addition, the loss function of the deep learning network was optimized with respect to two main objectives—accuracy and earliness—thereby improving model efficiency in producing more accurate and reliable maps. Finally, the data used in this research include the Sentinel-2 satellite images with a resolution of 10 and 20 m, which have been gathered in a time series form in different time intervals. The presented model (ELECTS) as a classifier network was trained by the desired data and then utilized to develop the updated plant cover maps (Rußwurm et al., 2023). Figure 2 shows a general scheme of the suggested method steps.

The used method is a time series classifier model involving the extractor of deep properties f_θ based on the recursion, which enters the time observations into the network and has two output decision-making branches. The used architecture in the first part is the recurrent neural networks (RNN), which can be implemented with

different architecture types of deep learning, but in the applied algorithm, the recurrent learning networks are focused on without losing the model generalization. RNN networks estimate a hidden view of h_t at time t based on a time series input like $X_{\rightarrow t} = (x_1, x_2, x_3, \ldots, x_t)$ from the observations x from the start time to t. The model can process the samples with different lengths and receive the time series with different lengths T as the inputs.

Therefore, it can produce the deep features h_t through receiving the network f_θ and the time series with the t member. Considering the occurrence of the derivative fading phenomenon in the recurrent learning networks, the recurrent LSTM is used as :

$$\{h_t, c_t\} = f_{\theta_h}(x_t, \{h_{t-1}, c_{t-1}\}) \quad (1)$$

which updates two representations simultaneously. Here, h_t is used in two branches differently. The first branch produces the probability of a pixel belonging to each class through

$$\hat{y}_t = \text{softmax}\left(f_{\theta_c}(h_t)\right) \quad (2)$$

and another one presents a numerical value as the probability of the algorithm stopping in the form of

$$d_t = \sigma\left(f_{\theta_d}(h_t)\right) \quad (3)$$

Here, σ refers to the sigmoid function that converts the stop branch output to a value between 0 and 1. After training the network and taking the final outputs, the value of the stop probability will be replaced by a specific threshold. For example, if the stop probability d_t equals 0.20, it will indicate the classification stops at time t with a probability of 20%. In practice, it can be observed that the speed of d_t will increase from 0 to 1 in a short time frame during the network training.

2.3. Loss function

Classification Loss is a mathematical function that measures the difference between the model's prediction and the actual output (correct label). Figure 3 shows a general scheme of the model, loss functions and relation number.

In this article, a recurrent network with the same parameters has been used for a set of data. A primary linear layer (normalizer layer) demonstrates the input data to a feature space with 32 dimensions at each time. In the following, two one-sided LSTM layers have been embedded in a network. At the end of the network in the decision-making branches, the sigmoid activation function for the decision of stopping or not stopping the model and the SoftMax function for the determination of the classification score have been considered. The general model has 67108 trainable parameters, leading to the network's lightness and trainable capability in every system with graphics. Adam optimization method with the learning rate of 0.001 and the release rate of 20% was used in this network. Determining the times of taking images around Ravansar was done based on the cloud cover amount in the reference time (2017), and afterwards, in the target year (2021), the times close to the available images with the cloud cover less than 5% were selected.

2.4. Training data migration

Collecting reference samples is a fundamental requirement of any monitored classification method. A lack of sufficient training samples is one of the main sources of error in classification algorithms. Collecting data through continuous and periodic ground surveys is time-consuming and costly. One recently proposed approach is the migration of reference training samples from a source time to appropriate target times. In this research, common training sample migration methods were investigated in terms of their formulation and performance using various datasets. In general, training sample migration methods consist of three basic stages:

1- the production of feature space,
2- the calculation of the difference (distance) between the samples
3- The determination of the optimal threshold limit; in the following, each stage will be addressed.

2.5. Feature space production

The sample spectrum contains comprehensive information about the inherent features of each class, enabling more precise separation of changed samples from unchanged ones. Different land-cover types have unique spectral signatures, and analyzing them across multiple wavelengths improves the effectiveness of distance-based measurement criteria and enhances sensitivity to environmental and temporal changes. This is particularly important in dynamic environments such as rangelands and agricultural areas, which are subject to seasonal and environmental variations. For non-plant classes, using sample spectra offers a significant advantage over plant indices, as the latter are typically sensitive only to specific plant traits, such as chlorophyll content, and are less effective in distinguishing non-plant classes. While plant indices cannot adequately separate spectral features of non-plant classes, such as soil and water, the use of the full spectral information allows for a more robust and comprehensive differentiation between plant and non-plant classes.

2.6. Selection of distance measurement criterion

The second stage in the migration of training data is to select the distance measurement criterion between the reference and target feature spaces. Most of the studies conducted by the researchers used spectral angular distance and Euclidean distance indices to compute the difference between the reference and target sample spectrums. In the current study, these criteria, along with

the DTW criterion, were investigated. Using the DTW index makes the estimate of spectral difference between the reference and target feature spaces possible with no consideration of time differences in the reference and target years. Thus, in the study, the performance of the three mentioned criteria is addressed in terms of training sample migration.

2.7. Selection of threshold

In the training data migration, the most important element is to make a decision to change or not to change the samples. According to the studies, a specific amount cannot be determined to separate the changed samples from the others (Sykas et al., 2022). Therefore, the best solution is to find the optimal threshold by trial and error. On the other hand, considering the scale difference in every feature space and every distance measurement criterion, a fixed threshold cannot be used for all the modes. Thus, it is essential to determine a threshold for each mode. In the present study, after calculating the distance, data were generated at reference and target times for different thresholds, and considering the final classification accuracy, an optimal threshold was determined for each case.

2.8. Validation criteria

In the field of remote sensing and machine learning, the classification accuracy is an important element in investigating the efficiency of a decision-making model (Chughtai et al., 2021). Evaluating the performance of classification models assures that the predictions are reliable and valid. Here, the total precision, recall, precision, Kappa, F-score were used to assess the classification precision.

3. Result

3.1. Euclidean distance criterion

In this section, the impact of different threshold limits on distance criteria in the spectral feature space was investigated using 10 Sentinel-2 bands. Tables 2 and 3 and Figures 4 and 5 present the results of training data migration using the Euclidean distance criterion and Sentinel-2 time series images. Based on the distribution of data in the feature space, threshold limits were selected according to the mean and standard deviation of the relevant data. The step size for adjusting threshold limits was set to 0.02, considering the data distribution and standard deviation. In the experiments, if there are sufficient training data, 2000 samples have been selected from each class for the training and validation. Total precision varies in the range of 0.60-0.76 and the best one occurred at the threshold of 0.20.

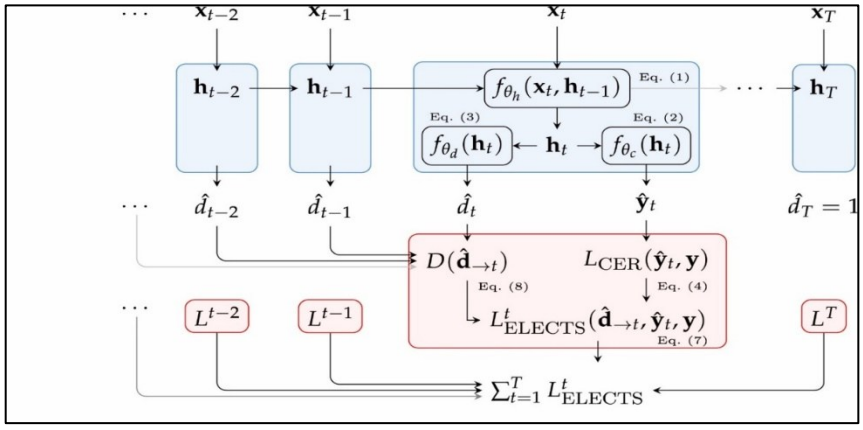

Figure 3. A scheme of model (blue) and loss functions (red). Arrows indicate the inputs and outputs

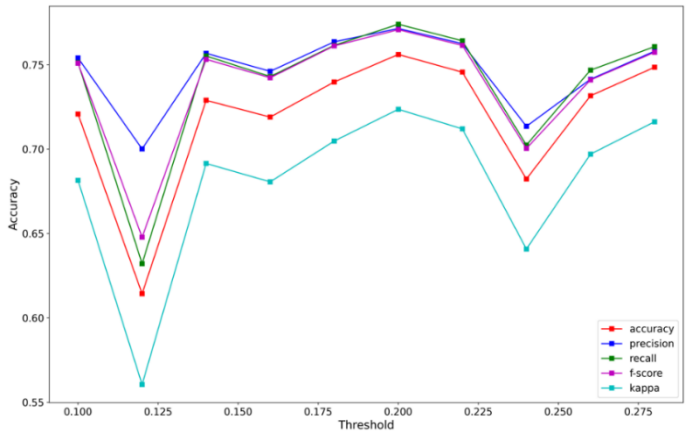

Figure 4. Behavior of precision criteria in training data classification based on the Euclidean distance calculation criterion

Table 2. Precision achieved based on different thresholds using the Euclidean distance calculation criterion

Threshold	Accuracy	Precision	Recall	F Score	Kappa	Earliness	Classification Loss
0.10	0.72	0.75	0.75	0.75	0.68	0.07	9.23
0.12	0.61	0.70	0.63	0.65	0.56	0.05	12.16
0.14	0.73	0.76	0.76	0.75	0.69	0.12	9.29
0.16	0.72	0.75	0.74	0.74	0.68	0.10	9.57
0.18	0.74	0.76	0.76	0.76	0.70	0.03	8.88
0.20	0.74	0.75	0.75	0.75	0.70	0.10	8.45
0.22	0.75	0.76	0.76	0.76	0.71	0.38	8.73
0.24	0.68	0.71	0.70	0.70	0.64	0.10	10.12
0.26	0.73	0.74	0.75	0.74	0.70	0.16	9.08
0.28	0.75	0.76	0.76	0.76	0.72	0.05	8.69

Table 3. Number of training data migrated based on different thresholds and Euclidean distance calculation criterion

Threshold	Migrated Samples	Urban	Rangelands	Farmland	Wetland	Kalut	Clay	Outcrop	Sand	Water
0.10	141425	28713	44188	34604	5373	5322	3257	12523	7226	219
0.12	188566	33684	54768	59452	5601	6323	3624	16204	8555	355
0.14	228875	36695	60105	84648	5712	7048	3860	20508	9799	500
0.16	262448	38546	63693	105622	5862	7915	4080	24945	11063	722
0.18	287522	39732	66622	119722	5940	8728	4305	29304	12235	934
0.20	304374	40561	69086	126836	5977	9346	4431	33711	13302	1124
0.22	317105	41111	71370	130620	6002	9933	4592	37998	14154	1325
0.24	327258	41444	72925	133304	6009	10333	4810	41920	14937	1576
0.26	335756	41703	73934	135770	6009	10528	4955	45431	15541	1885
0.28	342325	41876	74866	137896	6010	10600	5007	47968	15965	2137

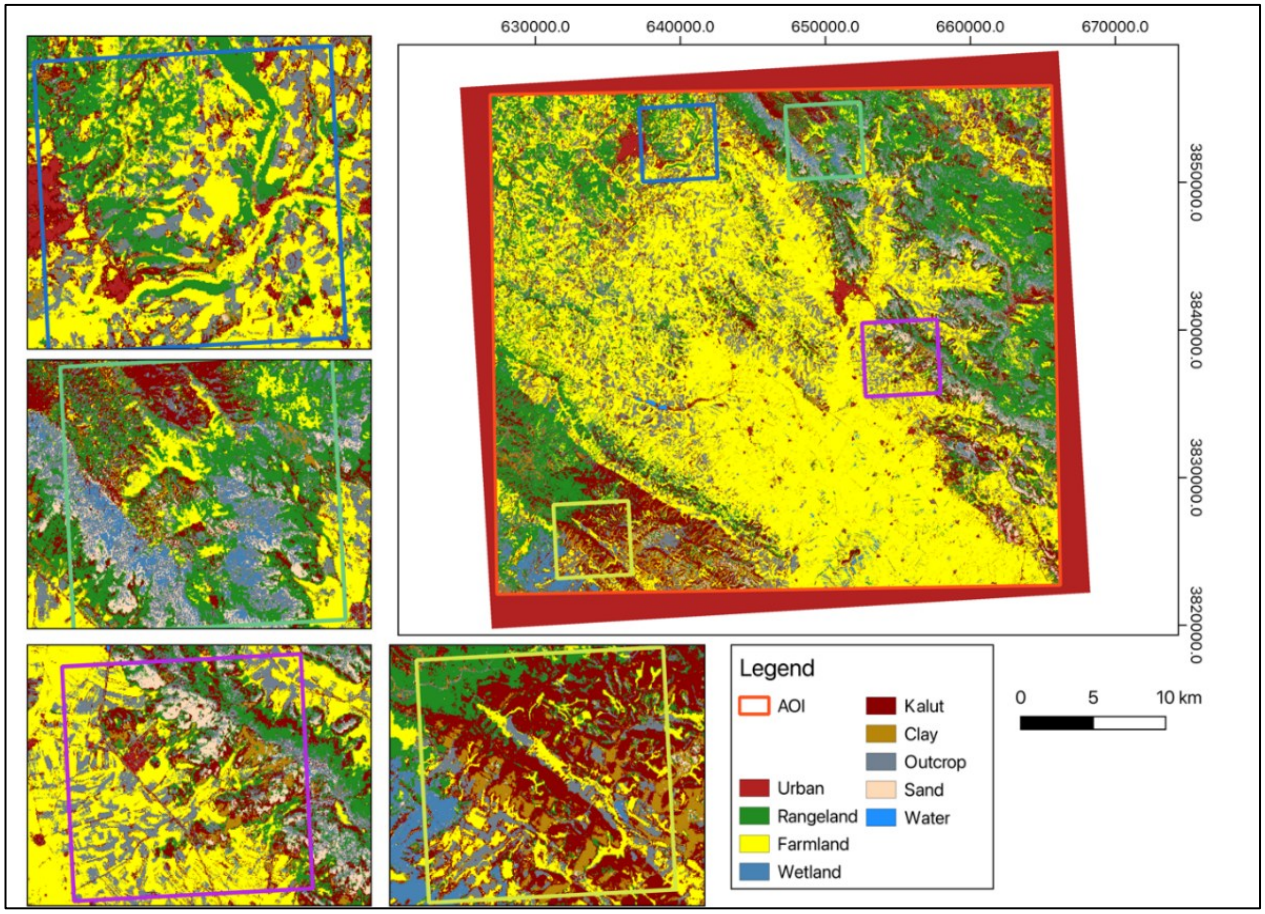

Figure 5. A map classified in 2021 based on the Euclidean distance criterion

10.57647/jrs.2026.1602.12

3.2. Spectral angular distance (SAD)

In this experiment, the spectral angular distance criterion and time series images were used in terms of training data migration. Like the previous experiment, the validation and training data and threshold limit were selected similarly. The threshold limits of 0.12-0.30 were investigated and as Figure 6 illustrates, the complexity of feature space has led to the fluctuation of model precision criteria in the threshold of 0.20. Total precision has fluctuated in most of the thresholds, but it reaches the peak given as 0.74 in the threshold of 0.24, demonstrating the most overlapping value between real and predicted data. In some thresholds like 0.20, the precision was significantly reduced to 0.12, indicating the threshold inefficiency in separating the classes appropriately.

Based on the analyses presented in Tables 4 and 5, a threshold of 0.24 was determined to be optimal, achieving the highest precision, the best alignment with evaluation criteria, and the lowest classification loss. Higher thresholds resulted in more migrated training samples, reflecting the model's ability to identify similar data across varying similarity levels. Therefore, a threshold of 0.24 was selected to balance evaluation and classification loss criteria while maximizing precision and accuracy. Figure 7 presents the map classified in 2021 using the SAD criterion.

3.3. Dynamic time warping (DTW)

In this experiment, the impact of different threshold limits on the migration of training data has been investigated by the DTW distance and a feature space consisting of the complication spectrum. Similar to the previous experiments, the threshold limits and steps were selected according to the mean and standard deviation of the desired data in the range of 0.1 to 0.3 (Figure 8). Also, training and validation data have been considered equally, and the characteristics and details were presented in Table 6.

Model precision started at 0.67 for a threshold of 0.10 and reached a maximum of 0.75 at a threshold of 0.30. Increasing the threshold improved model precision, indicating better performance at higher thresholds. Precision and recall generally ranged between 0.70 and 0.76, with their highest values observed at thresholds of 0.14 and 0.30. These results demonstrate the overall improvement of the model in recognizing target classes and reducing the error rate at medium and high thresholds. Table 7 indicates that the model achieves its best performance at a threshold of 0.14. Thresholds in the middle range allow the model to identify samples with high precision and accurately classify them. However, the table also shows that as the threshold increases, the number of misclassified (or migrated) samples grows, and the distribution of samples shifts noticeably in some classes. Figure 9 presents the classified map for 2021 based on the DTW criterion, while Figure 10 illustrates the results obtained using the most optimal threshold for each criterion.

4. Discussion

This research investigates the most effective criteria and settings for improving the migration of training samples in environmental studies. In machine learning applications, the migration of training samples depends on the training data volume, the distance calculation criterion, and its threshold, as these factors directly influence whether a sample is updated over time. The size of the training dataset affects the network training process: insufficient data can lead to inadequate model training, while an excessive amount of data can cause overfitting and reduce generalization. The choice of distance calculation criterion is also critical, as it interacts closely with the characteristics of the data and determines how sample matches and mismatches are identified. Finally, selecting an optimal threshold separates data branches effectively, resulting in a more generalizable and robust model. To examine the impact of each factor, a spectral curve-based feature space was employed, allowing the effects of these criteria to be systematically analyzed.

In comparing three criteria—Euclidean Distance (ED), Spectral Angle Distance (SAD), and Dynamic Time Warping (DTW)—for training sample migration, the results revealed that each criterion performs differently in transferring samples to the target time. ED is less sensitive to subtle differences in spectral properties due to its limited attention to complex spectral changes, resulting in lower accuracy in recognizing class transitions. It is particularly inefficient in areas with gradual changes and complex classes, such as plant cover, and transfers fewer samples correctly. In contrast, SAD captures spectral changes more precisely by measuring angles between spectral vectors, making it more accurate for classes with gradual changes like plant cover. However, its performance decreases in some non-plant areas. DTW, which accounts for time displacement and computes changes in multidimensional space, demonstrated high precision, especially for complex and variable classes. It transferred more samples correctly than both ED and SAD and performed well in both plant and non-plant areas. Therefore, DTW is identified as the most effective criterion for training sample migration in multidimensional feature spaces. Consequently, DTW is recommended for applications requiring high precision in recognizing complex classes, while SAD is suitable for estimating spectral changes in plant-dominated classes. To determine the optimal threshold for every criterion, a

network search was done to assess a variety of thresholds and to choose the best one. The optimization settings caused the migration of training samples to be performed more accurately and helped to decrease the error rate in the data. As a consequence, it is suggested to use the adaptive methods to determine the threshold based on the class type and spectral features for the optimization of model precision and the reduction of errors, so that each class will be analyzed by the suitable threshold.

After the migration of training data to the years 2017 and 2021, the data was entered into a deep learning network based on the time series. This network could produce highly precise theme maps using the updated data in 2021. These maps were able to be applied as a suitable tool to analyze and monitor the environmental changes in the case study.

This research indicated that the plant classes require more time data, while other classes need no time series. In addition, using the remote sensing data of the Sentinel-2 sensor for the migration of training samples from 2017 to 2021 indicated the efficiency of the proposed methods for producing the up-to-date maps without extensive land surveys. The proposed algorithm, which combines DTW, SAD, and ED distance measures with Sentinel-2 image time series and adaptive thresholds for different feature spaces, achieved an accuracy of up to 76%. Compared to other studies, the accuracy obtained using the dynamic temporal criterion with a threshold of 0.14 in spectral space (76%) is comparable to or higher than methods employing deep neural networks or more complex combinations of indicators. In similar studies, deep learning-based methods such as LSTM or CNNs have reported accuracy of around 80% to 90%, but often require a higher volume of data and computational time (Mazzia et al., 2019; Sefrin et al., 2020; Singh et al., 2022). In contrast, our method had achieved competitive accuracy by reducing computational complexity and using simpler distance criteria.

Table 4. Precision achieved based on different threshold limits using spectral angular distance calculation criterion

Threshold	Accuracy	Precision	Recall	Fscore	Kappa	Earliness	Classification Loss
0.12	0.73	0.65	0.65	0.65	0.69	0.08	9.33
0.14	0.67	0.61	0.60	0.60	0.63	0.19	10.65
0.16	0.72	0.75	0.70	0.72	0.68	0.29	9.44
0.18	0.73	0.76	0.66	0.67	0.69	0.41	9.20
0.20	0.12	0.14	0.11	0.06	0.00	0.00	21.74
0.22	0.73	0.74	0.71	0.72	0.69	0.11	9.65
0.24	0.74	0.76	0.76	0.76	0.71	0.09	9.31
0.26	0.73	0.72	0.74	0.73	0.69	0.09	9.66
0.28	0.69	0.73	0.72	0.72	0.64	0.08	11.02
0.30	0.67	0.71	0.70	0.70	0.63	0.21	11.30

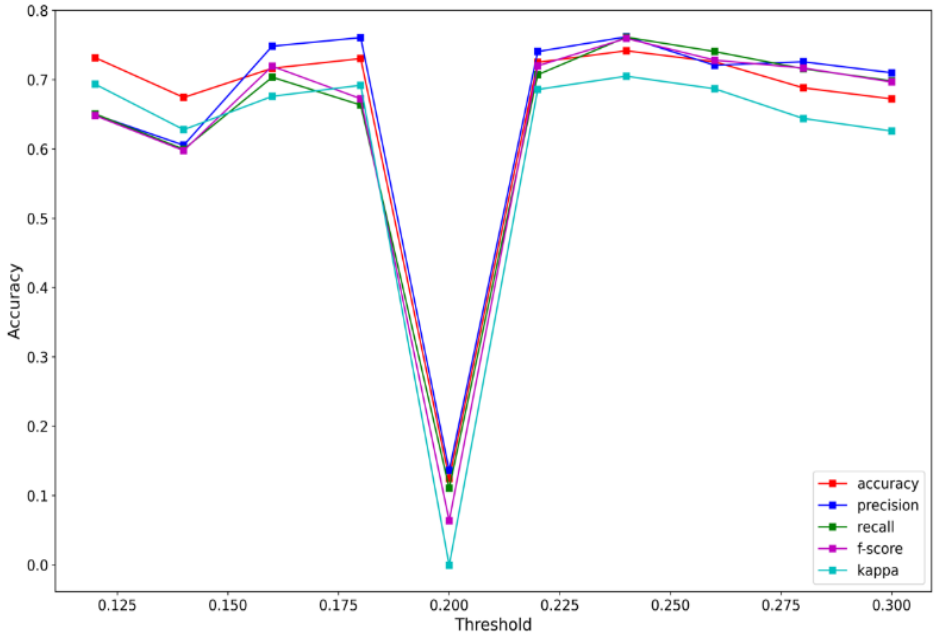

Figure 6. Behavior of precision criteria in the classification of training data based on spectral angular distance

10.57647/jrs.2026.1602.12

Table 5. Number of training data migrated based on different thresholds and spectral angular distance

Threshold	Migrated Samples	Urban	Rangelands	Farmland	Wetland	Kalut	Clay	Outcrop	Sand	Water
0.12	269684	42224	63006	100881	5744	9295	4986	28058	15488	2
0.14	286893	42265	64517	111428	5848	9687	5025	32037	16080	6
0.16	299307	42284	65994	118049	5910	9970	5049	35621	16421	9
0.18	309590	42300	67689	122691	5954	10225	5076	39012	16627	16
0.20	318344	42309	69409	126248	5976	10367	5115	42151	16745	24
0.22	325655	42315	71158	129104	5993	10399	5121	44709	16825	31
0.24	331396	42317	72624	131241	6003	10406	5124	46739	16893	49
0.26	335762	42321	73787	132827	6006	10409	5125	48282	16933	72
0.28	339192	42321	74703	133998	6009	10412	5125	49571	16950	103
0.30	342045	42324	75589	134992	6010	10418	5125	50478	16968	141

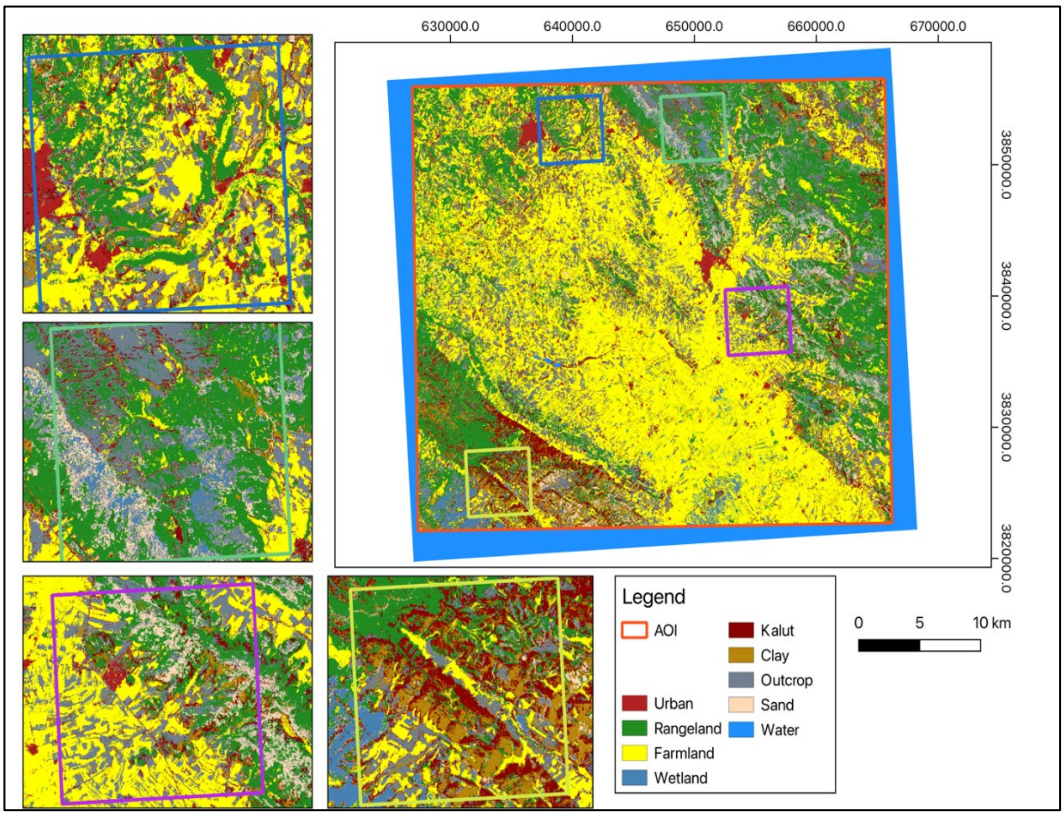

Figure 7. A map classified in 2021 based on Spectral Angular Distance

Table 6. The precision achieved by different thresholds using the DTW criterion

Threshold	Accuracy	Precision	Recall	Fscore	Kappa	Earliness	Classification Loss
0.10	0.67	0.71	0.70	0.70	0.63	0.10	10.32
0.12	0.73	0.74	0.74	0.74	0.69	0.14	9.08
0.14	0.75	0.76	0.76	0.76	0.71	0.16	8.94
0.16	0.73	0.74	0.74	0.74	0.69	0.14	9.64
0.18	0.71	0.72	0.73	0.72	0.68	0.15	9.53
0.20	0.72	0.74	0.73	0.73	0.68	0.12	10.14
0.22	0.68	0.72	0.70	0.70	0.64	0.19	9.81
0.24	0.73	0.74	0.74	0.73	0.69	0.07	9.23
0.26	0.72	0.74	0.73	0.73	0.68	0.07	9.45
0.28	0.74	0.75	0.75	0.75	0.71	0.19	8.97
0.30	0.75	0.76	0.76	0.76	0.72	0.15	8.80

10.57647/jrs.2026.1602.12

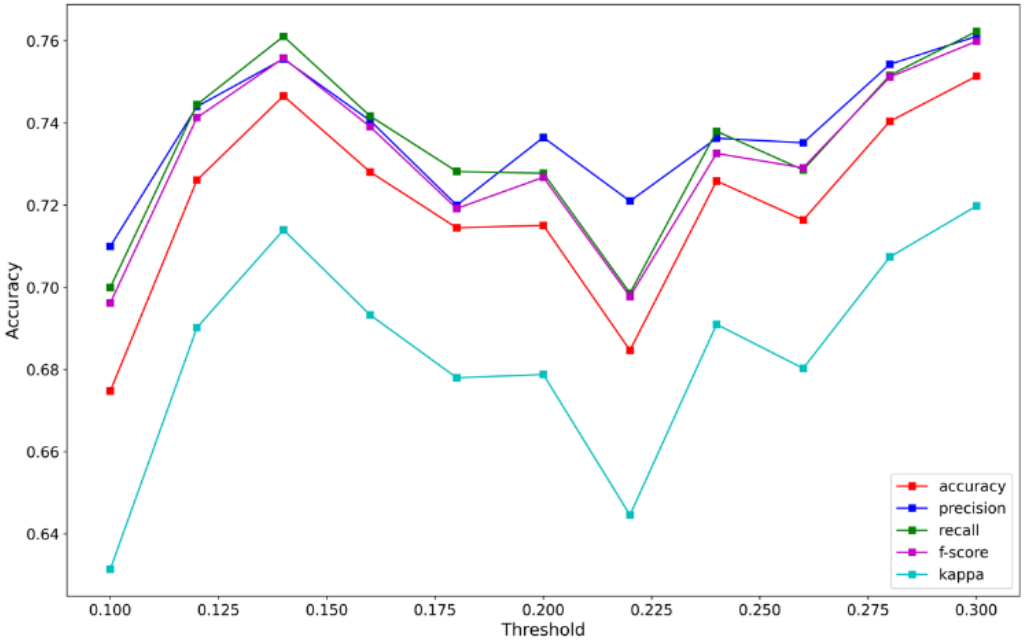

Figure 8. Behavior of precision criteria in the classification of training data according to the DTW distance calculation criterion

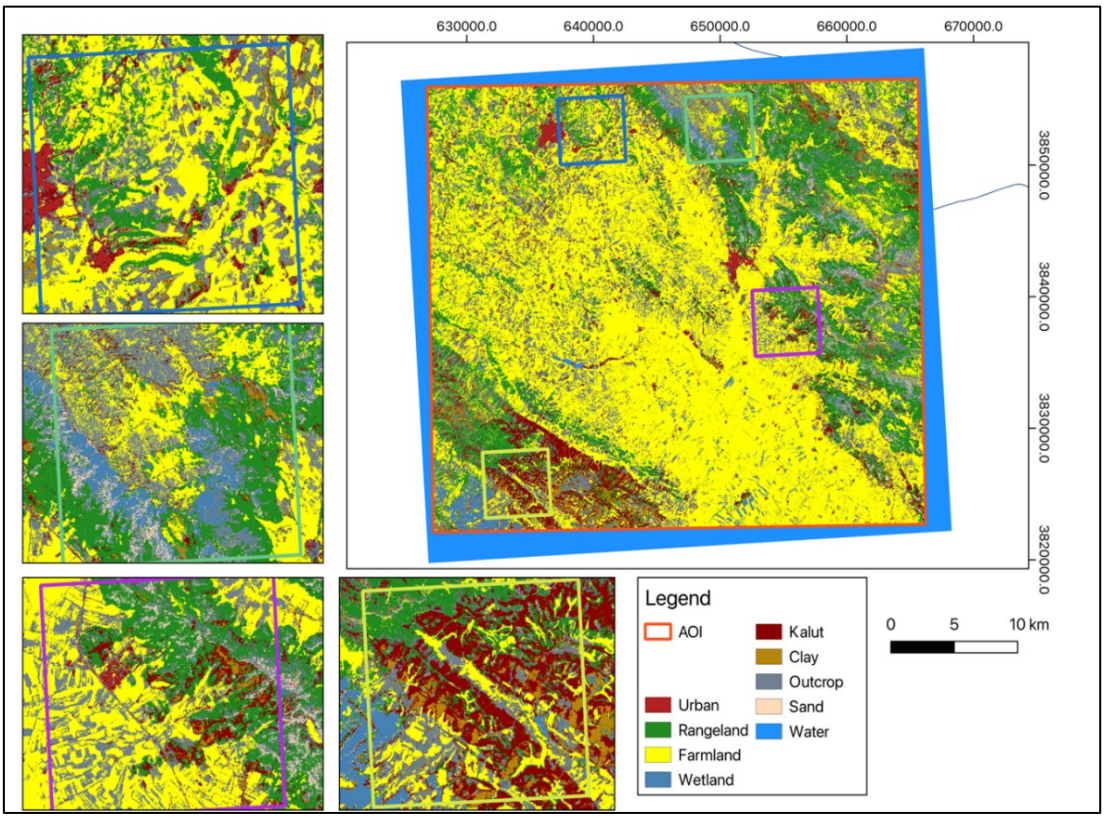

Figure 9. The Classified map in 2021 based on the DTW criterion

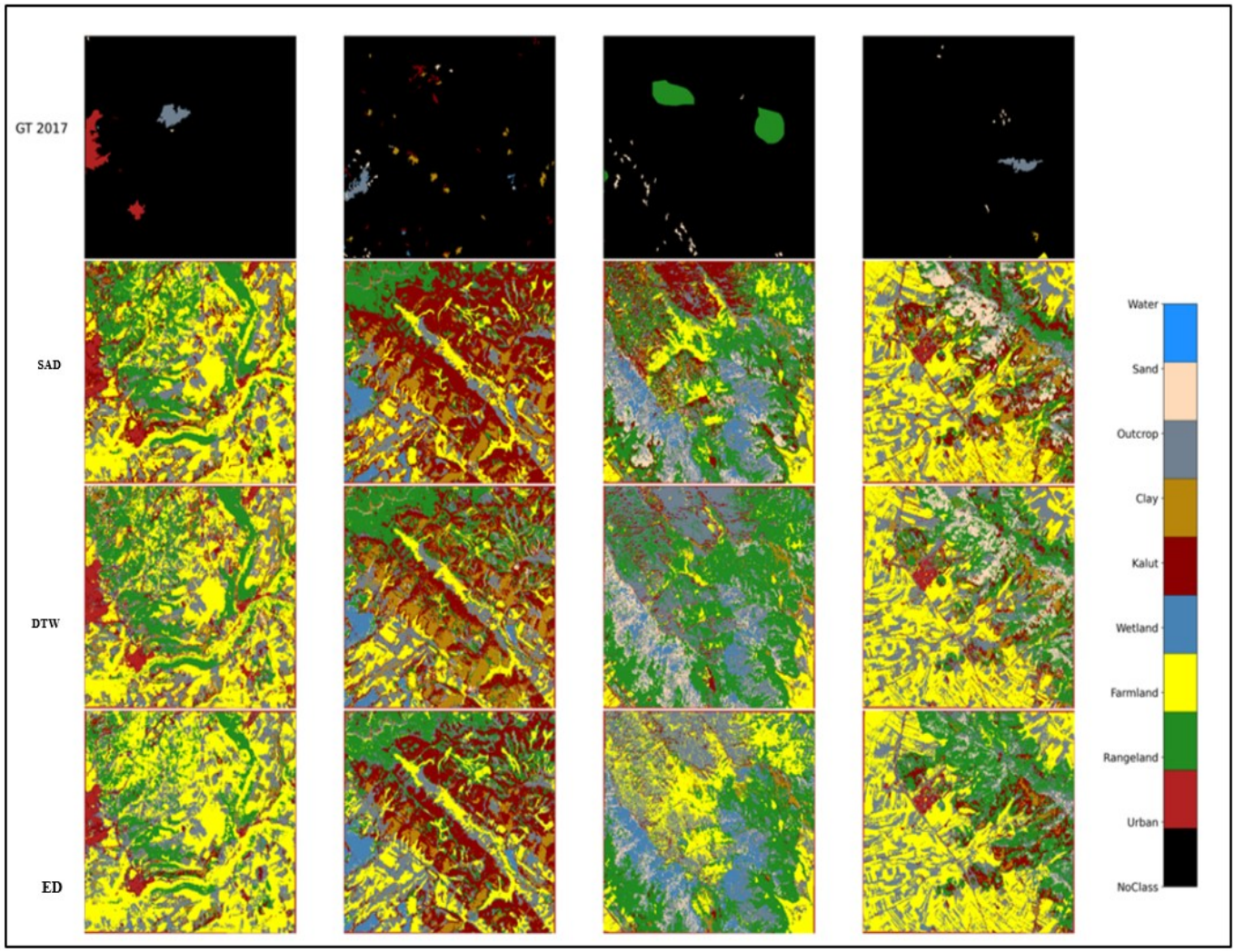

Figure 10. Results of classification based on the most optimal threshold for each distance calculation criterion in 2021

Table 7. Number of migrated data according to different thresholds and the DTW criterion

Threshold	Migrated samples	Urban	Rangelands	Farmland	Wetland	Kalut	Clay	Outcrop	Sand	Water
0.10	261152	38004	63288	104949	5820	8455	4186	24432	10922	1096
0.12	297916	40392	67333	123889	5959	9463	4412	32041	12922	1505
0.14	320934	41442	70389	132038	5991	10230	4606	39898	14431	1909
0.16	334653	41874	72452	135926	6001	10503	4829	45519	15395	2154
0.18	342086	42058	73961	137721	6008	10608	4978	48520	15980	2252
0.20	346622	42138	75070	138631	6010	10654	5036	50370	16349	2364
0.22	349296	42200	75990	139113	6010	10678	5107	51228	16564	2406
0.24	351003	42230	76722	139436	6010	10689	5115	51668	16727	2406
0.26	352353	42258	77444	139587	6010	10695	5121	51975	16857	2406
0.28	353551	42276	78219	139665	6010	10700	5124	52202	16949	2406
0.30	354526	42290	78896	139747	6010	10702	5125	52334	17016	2406

5. Conclusion

Training sample migration method for classification provides valuable insights into the changes and dynamics of plant covers, alongside the identification and classification of vegetation, which are vital for the optimal management of natural resources and food security. The

final map, which integrates plant cover and other classes, provides a practical tool for monitoring annual vegetation changes and assessing ecological shifts, supporting policymakers and researchers in strategic planning and management. Our findings indicate that applying deep learning algorithms to model time series dynamics and leverage long-term information can significantly improve vegetation classification accuracy. In particular, models such as LSTM demonstrate a strong ability to capture complex patterns from time series data, enhancing classification performance.

Authors Contribution

All the authors have participated sufficiently in the intellectual content, conception and design of this work or the analysis and interpretation of the data (when applicable), as well as the writing of the manuscript.

Availability of data and materials

The data that support the findings of this study are available from the corresponding author, upon reasonable request.

Conflict of interests

The author states that there is no conflict of interest.

References

Conant, R. T. 2010. Challenges and opportunities for carbon sequestration in grassland systems (Vol. 9). FAO, Rome, Italy. https://www.fao.org/fileadmin/templates/agphome/documents/climate/AGPC_grassland_webversion_19.pdf

Chughtai, A. H., Abbasi, H., & Karas, I. R. 2021. A review of the change detection method and accuracy assessment for land use cover. Remote Sensing Applications: Society and Environment, 22, 100482. https://doi.org/10.1016/j.rsase.2021.100482

Delince, J., Lemoine, G., Defourny, P., Gallego, J., Davidson, A., Ray, S., Rojas, O., Latham, J., & Achard, F. 2017. Handbook on remote sensing for agricultural statistics. GSARS: Rome, Italy. https://openknowledge.fao.org

Fekri, E., Latifi, H., Amani, M., & Zobeidinezhad, A. 2021. A training sample migration method for wetland mapping and monitoring using Sentinel data in Google Earth Engine. Remote Sensing, 13(20), 4169. https://doi.org/10.3390/rs13204169

Garnot, V.S.F., Landrieu, L., Giordano, S. and Chehata, N. 2020. Satellite Image Time Series Classification with Pixel-Set Encoders and Temporal Self-Attention. Proceedings of the IEEE/CVF Conference on Computer Vision and Pattern Recognition, Seattle, 13-19 June 2020, 12325-12334.

Ghorbanian, A., Kakooei, M., Amani, M., Mahdavi, S., Mohammadzadeh, A., & Hasanlou, M. 2020. Improved land cover map of Iran using Sentinel imagery within Google Earth Engine and a novel automatic workflow for land cover classification using migrated training samples. ISPRS Journal of Photogrammetry and Remote Sensing, 167, 276-288. https://doi.org/10.1016/j.isprsjprs.2020.07.013

Ghorbanian, A., Zaghian, S., Asiyabi, R. M., Amani, M., Mohammadzadeh, A., & Jamali, S. 2021. Mangrove ecosystem mapping using Sentinel-1 and Sentinel-2 satellite images and a random forest algorithm in Google Earth Engine. Remote Sensing, 13(13), 2565. https://doi.org/10.3390/rs13132565

Gibon, A. 2005. Managing grassland for production, the environment and the landscape. Challenges at the farm and the landscape level. Livestock Production Science, 96(1), 11-31. https://doi.org/10.1016/j.livprodsci.2005.05.009

Guo, M., Li, J., Sheng, C., Xu, J., & Wu, L. 2017. A review of wetland remote sensing. Sensors, 17(4), 777. https://doi.org/10.3390/s17040777

Hilpold, A., Seeber, J., Fontana, V., Niedrist, G., Rief, A., Steinwandter, M., Tasser, E., & Tappeiner, U. 2018. Decline of rare and specialist species across multiple taxonomic groups after grassland intensification and abandonment. Biodiversity and Conservation, 27(14), 3729-3744. https://doi.org/10.1007/s10531-018-1623-x

Lengyel, S., Déri, E., & Magura, T. 2016. Species richness responses to structural or compositional habitat diversity between and within grassland patches: a multi-taxon approach. PLoS One, 11(2), e0149662. https://doi.org/10.1371/journal.pone.0149662

Mao, D., Wang, Z., Du, B., Li, L., Tian, Y., Jia, M., Zeng, Y., Song, K., Jiang, M., & Wang, Y. 2020. National wetland mapping in China: A new product resulting from object-based and hierarchical classification of Landsat 8 OLI images. ISPRS Journal of Photogrammetry and Remote Sensing, 164, 11-25. https://doi.org/10.1016/j.isprsjprs.2020.03.020

Mariotto, I., Thenkabail, P. S., Huete, A., Slonecker, E. T., & Platonov, A. 2013. Hyperspectral versus multispectral crop-productivity modeling and type discrimination for the HyspIRI mission. Remote Sensing of Environment, 139, 291-305. https://doi.org/10.1016/j.rse.2013.08.002

Mazzia, V., Khaliq, A., & Chiaberge, M. 2019. Improvement in land cover and crop classification based on temporal features learning from Sentinel-2 data using recurrent-convolutional neural network (R-CNN). Applied Sciences, 10(1), 238. https://doi.org/10.3390/app10010238

Rapinel, S., Rossignol, N., Gore, O., Jambon, O., Bouger, G., Mansons, J., & Bonis, A. 2018. Daily monitoring of shallow and fine-grained water patterns in wet grasslands combining aerial LiDAR data and in situ piezometric measurements. Sustainability, 10(3), 708. https://doi.org/10.3390/su10030708

Reichstein, M., Ciais, P., Papale, D., Valentini, R., Running, S., Viovy, N., Cramer, W., Granier, A., Ogée, J., & Allard, V. 2007. Reduction of ecosystem productivity and respiration during the European summer 2003 climate anomaly: a joint flux tower, remote sensing and modelling analysis. Global Change Biology, 13(3), 634-651. http://dx.doi.org/10.1111/j.1365-2486.2006.01224.x

Reinermann, S., Asam, S., & Kuenzer, C. 2020. Remote sensing of grassland production and management—A review. Remote Sensing, 12(12), 1949. https://doi.org/10.3390/rs12121949

Reynolds, S., Frame, J. 2005. Grasslands: developments, opportunities, perspectives. CRC Press.Grasslands: Developments, Opportunities, Perspectives - Google Books

Rußwurm, M., Courty, N., Emonet, R., Lefèvre, S., Tuia, D., & Tavenard, R. 2023. End-to-end learned early classification of time series for in-season crop type mapping. ISPRS Journal of Photogrammetry and Remote Sensing, 196, 445-456. https://doi.org/10.1016/j.isprsjprs.2022.12.016

Rußwurm, M., & Körner, M. 2018. Multi-temporal land cover classification with sequential recurrent encoders. ISPRS International Journal of Geo-Information, 7(4), 129. https://doi.org/10.3390/ijgi7040129

Rußwurm, M., & Körner, M. 2020. Self-attention for raw optical satellite time series classification. ISPRS Journal of Photogrammetry and Remote Sensing, 169, 421-435. https://doi.org/10.1016/j.isprsjprs.2020.06.006

Sefrin, O., Riese, F. M., & Keller, S. (2020). Deep learning for land cover change detection. Remote Sensing, 13(1), 78. https://doi.org/10.3390/rs13010078

Singh, G., Singh, S., Sethi, G., & Sood, V. (2022). Deep learning in the mapping of agricultural land use using Sentinel-2 satellite data. Geographies, 2(4), 691-700. https://doi.org/10.3390/geographies2040042

Sykas, D., Sdraka, M., Zografakis, D., & Papoutsis, I. 2022. A Sentinel-2 multiyear, multicounty benchmark dataset for crop classification and segmentation with deep learning. IEEE Journal of Selected Topics in Applied Earth Observations and Remote Sensing, 15, 3323-3339. https://doi.org/10.48550/arXiv.2204.00951

White, R.P., Murray, S. and Rohweder, M. (2000) Pilot Analysis of Global Ecosystems: Grassland Ecosystems. World Resources Institute, Washington DC, 81 p. http://pdf.wri.org/page_grasslands.pdf

Zhang, S., Yang, J., Leng, P., Ma, Y., Wang, H., & Song, Q. 2023. Crop type mapping with temporal sample migration. International Journal of Remote Sensing, VOL. 45, NOS. 19–20, 7014–7032. https://doi.org/10.1080/01431161.2023.2192881

Zhang, S., Yang, J., Leng, P., Ma, Y., Wang, H., & Song, Q. 2023. Crop type mapping with temporal sample migration. International Journal of Remote Sensing, 2024, VOL. 45, NOS. 19–20, 7014–7032